Editors' Suggestion

Precision Measurement of the $n=2$ Triplet P $J=1$ to $J=0$ Fine Structure of Atomic Helium Using Frequency-Offset Separated Oscillatory Fields

F. Heydarizadmotlagh, T. D. G. Skinner, K. Kato, M. C. George, and E. A. Hessels*
Department of Physics and Astronomy, York University, Toronto, Ontario M3J 1P3, Canada

(Received 20 November 2023; accepted 28 February 2024; published 19 April 2024)

Increasing accuracy of the theory and experiment of the $n = 2$ ^{3}P fine structure of helium has allowed for increasingly precise tests of quantum electrodynamics (QED), determinations of the fine-structure constant α, and limitations on possible beyond the standard model physics. Here we present a 2 ppb measurement of the $J = 1$ to $J = 0$ interval. The measurement is performed using frequency-offset separated-oscillatory fields. Our result of 29 616 955 018(60) Hz represents a landmark for helium fine-structure measurements, and, for the first time, will allow for a 1-ppb determination of the fine-structure constant when QED theory for the interval is improved.

DOI: 10.1103/PhysRevLett.132.163001

In 1964 Schwartz suggested [1] that the $n = 2$ ^{3}P states of helium could allow for a more precise determination of the fine-structure constant α than could be derived from studying the 2P fine structure of hydrogen, given that helium has a 60 times longer lifetime and a 3 times larger interval. He suggested that a part-per-million determination of α might be possible if improvements were made in both theory and experiment. In the intervening decades, experimental measurements have shown continual improvements [2–22]. The evaluation of new systematic effects [23–27] has improved the agreement between these measurements. Quantum-electrodynamic (QED) theory [28–51] for these intervals has also advanced greatly with a complete calculation of all terms of order α^6 (times mc^2) [34] in 1972, and all terms of order α^7 being completed [48] in 2010. This improved theoretical precision and the 4 orders of magnitude of improved experimental precision since 1965 [52] are illustrated in Fig. 6 (in the Supplemental Material [53]).

We present here a measurement of the $2^3\mathrm{P}_1 \to 2^3\mathrm{P}_0$ interval that has an uncertainty of only 2 parts per billion (ppb). This work is the experimental contribution towards using the 2^3P fine structure for tests of physics and fundamental constants at the ppb level. An advance of QED theory to this same level of accuracy will require a full calculation of all terms of order α^8.

A ppb-level comparison between experiment and QED calculations will have wide-ranging implications. It will provide the most accurate test to date of QED in a multielectron system [54]. This comparison will allow the 2^3P fine structure to be used for a direct test for beyond the standard model physics [54], such as exotic spin-dependent interactions between electrons [55] (at 100 times the accuracy of current tests). Finally, the combination of a complete calculation to order α^8 and our current measurement will allow for a determination of α at a level of 1 ppb—1000 times more accurate than the proposal of Schwartz [1]. The best determinations of α, based on the electron magnetic moment (g_e) [56–60] and atomic recoil [61,62], currently show discrepancies of more than 1 ppb (see Fig. 7 in the Supplemental Material [53]). Comparison of determinations of α obtained from various systems allows for tests of beyond the standard model physics in each of the systems [56,63–65].

Many aspects of our measurement apparatus (Fig. 1) are similar to those used [22] for our measurement of the $2^3\mathrm{P}_2 \to 2^3\mathrm{P}_1$ interval. A cryogenic beam of metastable 2^3S helium atoms with a mean speed of 1100 m/s is created in a dc discharge and is intensified (to a flux of $7 \times 10^{12}/\mathrm{cm}^2/\mathrm{s}$) by a two-dimensional magneto-optical trap (2DMOT). The atoms are optically pumped (see Fig. 1) into the $2^3\mathrm{S}(m = -1)$ state before passing through a rectangular microwave waveguide (WR-28, with inner dimensions of 7.112 by 3.556 mm, with 0.5-mm-diameter holes through which the beam enters and exits). Inside this waveguide, the majority of the $2^3\mathrm{S}(m = -1)$ atoms are excited by a pulse of 1083-nm laser light (laser A in Fig. 1, focused to 1 mm) to the $2^3\mathrm{P}_1(m = 0)$ state, which has a lifetime of 98 ns. The $2^3\mathrm{P}_1(m = 0) \to 2^3\mathrm{P}_0(m = 0)$ transition is then driven with 29.6-GHz microwaves. The resulting $2^3\mathrm{P}_0$ atoms are detected via excitation to $4^3\mathrm{D}_1$ using a pulse of 447-nm laser light (B in Fig. 1), and then to $18^3\mathrm{P}_2$ using a pulse of 1532-nm light (C in Fig. 1). The $18^3\mathrm{P}_2$ atoms are Stark-ionized by electric fields [see Fig. 1(c)], with the resulting ions being collected.

The microwave transition is driven with two pulses, each of duration D, and separated in time by T, as shown in Fig. 1(d). In the ~1 μs that it takes for the atoms to pass through the laser beams, they typically experience one or two cycles of the timing sequence of Fig. 1(d). These pulses are created by fast switching of microwaves output from

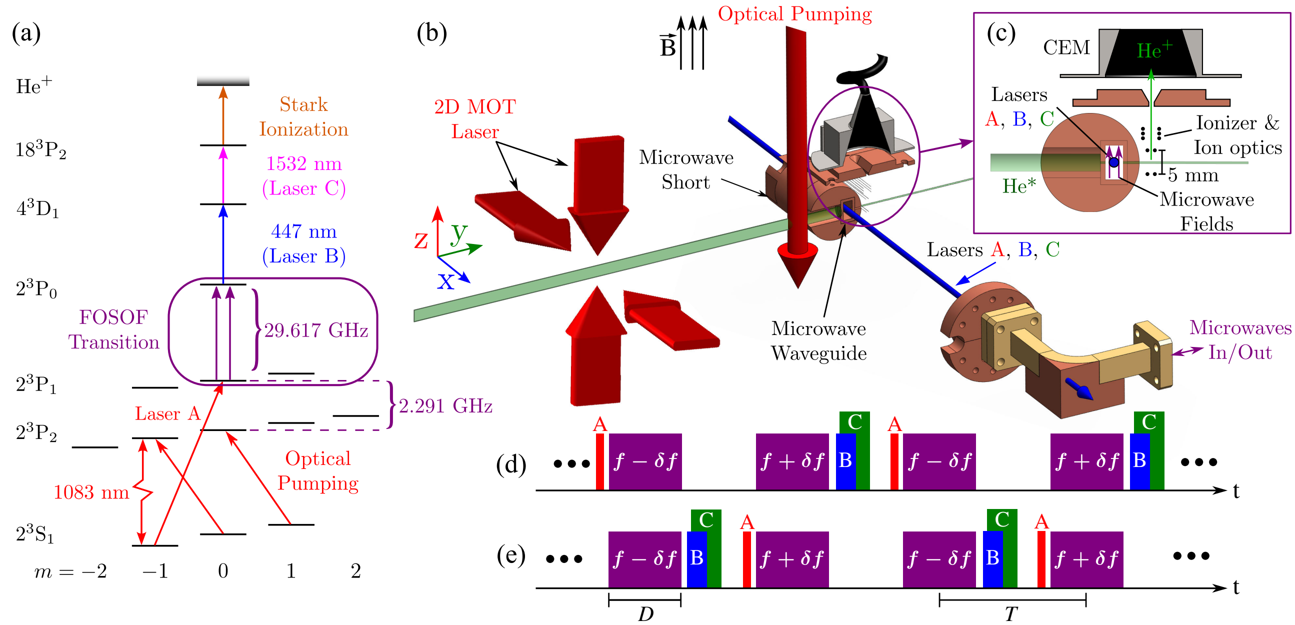

FIG. 1. The experimental setup. An energy-level diagram (a), (not to scale) shows the 29.617-GHz interval being measured and the laser transitions used for optical pumping and for the three laser pulses (A, B, C). The experimental setup (b), along with an expanded view of the region where the measurement takes place (c), shows the laser and microwave interactions and ionization detection. The timing diagrams, (d) and (e), show the laser and FOSOF microwave pulses for the two timing sequences used.

two precision generators, with their internal clocks locked to each other and referenced to both Rb and GPS clocks. The amplified microwaves (of power $P \leq 2$ W) enter one end of the waveguide and reflect off of a short that is situated one half wavelength from the 0.5-mm holes. The result is a standing wave that has an antinode of magnetic field and a node of electric field along the center line of the atomic beam.

The current work uses the frequency-offset separated-oscillatory-fields (FOSOF) technique [66], which is a modification of the Ramsey method [67] of separated oscillatory fields (SOF). Alternate microwave pulses have frequencies $f+\delta f$ and $f-\delta f$ [Fig. 1(d)]. The offset frequency $2\delta f$ (typically 280 Hz) causes the relative phases of the two pulses to vary continuously in time. As a result, the atomic signal [see Fig. 2(a)] cycles between destructive and constructive interference. The phase difference $\Delta\theta$ between this signal and a beat signal, obtained by combining the microwaves at the two frequencies, is indicated in Fig. 2(a). Data are taken with two different timing sequences: Fig. 1(d), in which the $f+\delta f$ pulse occurs before the $f-\delta f$ pulse, and Fig. 1(e), in which this ordering is reversed. To switch from (d) to (e), only the timing of the laser pulses is shifted—the microwave pulses remain unchanged. Figure 2(a) shows that the sign of the phase shift $\Delta\theta$ is opposite for the two cases. The quantity $\overline{\Delta\theta} = (\Delta\theta_{(\mathrm{d})} - \Delta\theta_{(\mathrm{e})})/2$ cancels unintended phase shifts in both the atomic and beat signals, as discussed in Ref. [66].

For a two-level system with two ideal pulses of duration D and separation T, the FOSOF line shape is

$$\overline{\Delta\theta}(f) = \Delta\omega(T-D) + 2\arctan\left[\frac{\Delta\omega\tan(\sqrt{4V^2+\Delta\omega^2}D/2)}{\sqrt{4V^2+\Delta\omega^2}}\right], \quad (1)$$

where V is the magnetic-dipole matrix element driving the transition, and $\Delta\omega/2\pi = f - f_0$ is the detuning of the applied microwave frequency from the atomic resonant frequency. This line shape is antisymmetric with respect to $\Delta\omega$ (with $\overline{\Delta\theta} = 0$ at $\Delta\omega = 0$), and reduces to the very simple proportional relation $\overline{\Delta\theta} = \Delta\omega T$ for small V. The observed line shape is shown in Fig. 2(b) for the case of $T = 300$ ns and $D = 100$ ns for three different values of V (i.e., different powers P). The line shapes are very nearly described by the $\Delta\omega T$ linear expression. On a 300-times expanded scale in Fig. 2(c), where the $\Delta\omega T$ straight line is subtracted, one can see that the data is described well by the line shape of Eq. (1).

A fit to $\overline{\Delta\theta}$ data taken at a set of microwave frequencies (ordered randomly) and at 100% power (corresponding to $V = 2.03$ rad/μs) gives an f_0 determination with an uncertainty of only 13 Hz. The residuals from this fit, shown in Fig. 2(f), are 100 000 times smaller than the range shown in Fig. 2(b), indicating that the line shape is understood at this level. The data in the figure are the average of many repetitions of the measurements taken at various times that span six months of data collection, with

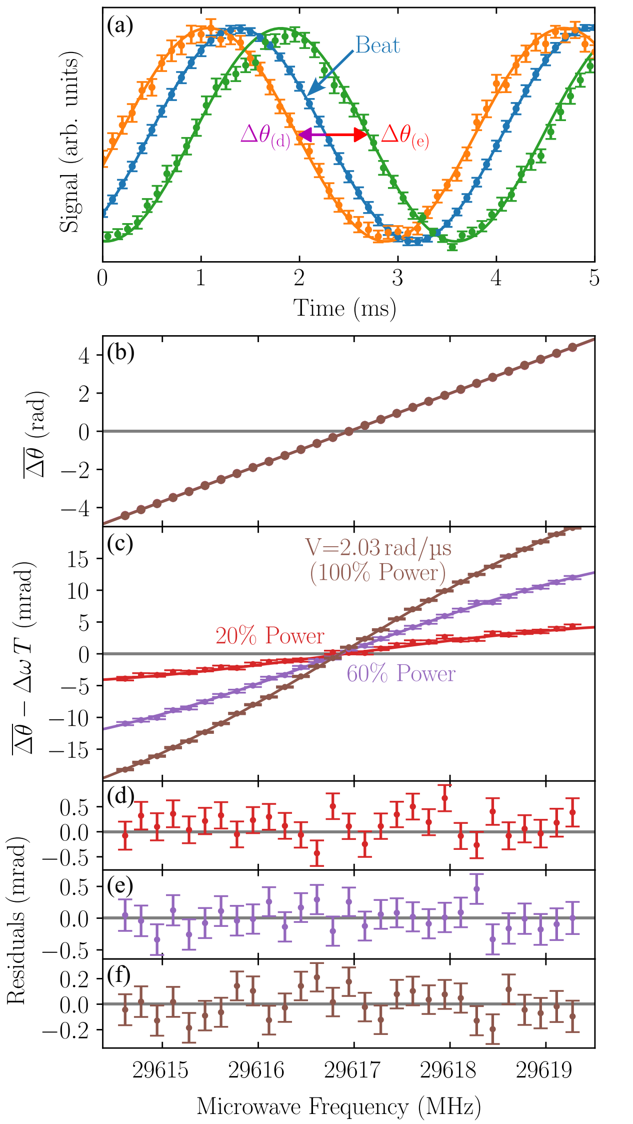

FIG. 2. The FOSOF line shape. The sinusoidal atomic signals for the configurations of Figs. 1(d) and 1(e) are shifted by $\Delta\theta_{(d)}$ and $\Delta\theta_{(e)}$ relative to a microwave beat signal, as shown in (a). $\overline{\Delta\theta} = (\Delta\theta_{(d)}) - \Delta\theta_{(e)})/2$ is shown in (b). A 300 times expanded scale in (c), where $\Delta\omega T$ is subtracted, resolves the line shapes for different powers. The fits in (c) use Eq. (1), and the residuals from the fits are shown in (d),(e), and (f).

individual points being averages of a total of 100 min of data. The excellent signal-to-noise ratio is despite the fact that the measurement sequence takes 450 ns, allowing only $e^{-(450\ \mathrm{ns})/(98\ \mathrm{ns})} = 1.0\%$ of the 2^3P atoms to contribute to the signal. The improved statistics (cf. Ref. [18]) is mostly due to the 2DMOT and the high efficiency of our Stark-ionization detection.

Equation (1) assumes ideal microwave pulses, including instantaneous turn-on and turn-off, no chirp in the phase due to the microwave switches or amplifier, and no changes in intensity or phase profiles as a function of f. Extensive

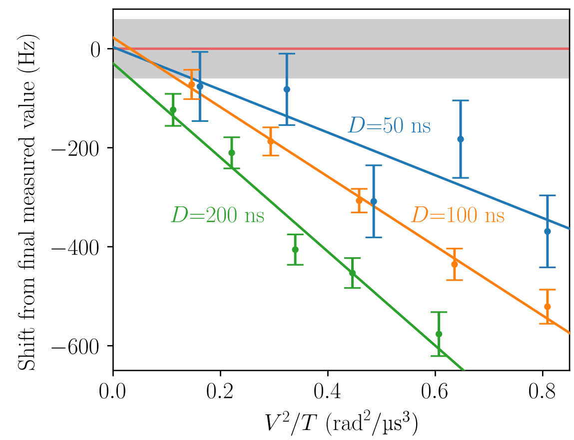

FIG. 3. The extrapolation of the averaged $D = 200$, $D = 100$, and $D = 50$ ns FOSOF fit centers to $P = 0$, where the center is unaffected by imperfections in the pulses. The extrapolated centers, along with their uncertainties, are shown in Fig. 4(d). The gray band represents the final uncertainty for the present measurement.

modeling shows that all forms of distortion give shifts that are proportional to P (that is, shifts that extrapolate exactly to zero in the zero-power limit). Therefore, we linearly extrapolate our measured FOSOF centers [from fits to Eq. (1), as in Fig. 2] to $P = 0$, as shown in Fig. 3. These extrapolations also account for very small ac Zeeman and ac Stark shifts caused by the microwaves. Both modeling and measurements show that the slopes for these extrapolations are nearly proportional to D/T. Measurements are repeated for various combinations of T and D to confirm that all sets of parameters extrapolate to a single intercept, as shown in Figs. 4(b)–4(d). Both in Ref. [22] and the current work, some data are taken with different levels of imperfections (and therefore slopes that differ by a factor of approximately three), and these still resulted in consistent intercepts within the accuracy of the tests.

Our experiment is performed within a magnetic field $\vec{B}$ of 5 G, which is applied by 20-cm-diameter Helmholtz coils. Before applying this field, the local magnetic field is canceled using six larger coils. This cancellation is calibrated by comparing the magnitude of the Zeeman shifts of our 2^3P intervals when positive and negative fields are applied. The largest systematic correction in our measurement is a second-order Zeeman shift of 197.74 Hz/G^2, which has been carefully studied (at the $< 0.01\%$ level of accuracy) by theory [68], and experiment [15,69]. We also use larger B to directly show that we understand the magnetic shifts at a level of $< 0.1\%$, and we include a 0.1% uncertainty to all Zeeman corrections. Figure 4(a) shows that measurements taken with $\vec{B}$ in the $+\hat{z}$ and $-\hat{z}$ directions agree, and that those with $|\vec{B}| = 5$ G agree with those taken for $|\vec{B}| = 10$ and $|\vec{B}| = 15$ G (which have 4 and 9 times larger Zeeman shifts, respectively).

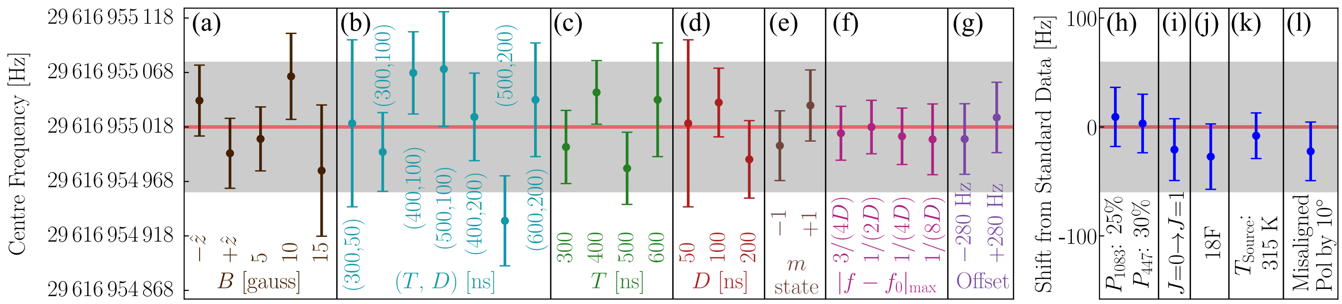

FIG. 4. A summary of the average obtained center value for the various values of the experimental parameters. All points are extrapolations to zero power and use the frequency range $|f - f_0| < 1/(2D)$, unless otherwise specified. As further discussed in the text, parts (a) through (g) show the average line centers for different B, T, D, m, $|f - f_0|$, and offset frequency and parts (h) through (l) show shifts of line centers (for $T = 300$, $D = 100$ ns, and 100% power) obtained with nonstandard parameter values (compared to similar line centers with standard parameter values). The gray band represents the final uncertainty for the present measurement.

The Doppler shift is small due to both the slow speed (1100 m/s) of our atoms (measured by the time-of-flight delay after passing through a mechanical chopper) and the fact that the microwaves travel in a direction that is perpendicular (to within 5 mrad) to the velocity of the atoms. The Doppler shift is further reduced by reflecting the microwaves from a short and having them intersect the atomic beam a second time. Ohmic heating by the microwaves of the gold-plated waveguide is calculated to lead to a difference of only 0.4% for power of the reflected microwaves. The net Doppler shift, after taking these factors into account, is zero with an uncertainty of ± 2 Hz.

The polarization for the optical-pumping step is reversed for half of the measurements, leading to a starting population in the $2^3\mathrm{S}(m = +1)$ state. Figure 4(e) shows that consistent results are obtained with $m = +1$ and -1. To test for possible FOSOF line shape effects, the data are refit with only the central frequencies [$|f - f_0| < 1/(2D)$, $1/(4D)$, or $1/(8D)$] included in the fit. Consistent results are found, as shown in Fig. 4(f). Figure 4(g) shows that the result does not depend on the sign of the offset frequency.

To test for light shifts due to unintended temporal overlap of the laser and microwave pulses, data are taken at lower powers for the 447 and 1083-nm lasers. As shown in Fig. 4(h), no shifts are seen. The fact that the same result is obtained [Fig. 4(i)] when driving the $J = 1$ to $J = 0$ and $J = 0$ to $J = 1$ (by retuning lasers A and B of Fig. 1) and when using a different Rydberg state [the $18^3\mathrm{F}$ state, Fig. 4(j)], indicates that unintended atomic processes are not affecting the measurement. A warmer source temperature (315 K, cf. 130 K), and hence a faster atomic beam, also reveals no inconsistency, as seen in Fig. 4(k). Finally, intentionally misaligning the linear polarization of laser A of Fig. 1 by 10° away from perpendicular to the applied $\vec{B}$ field leads to no change in the center [Fig. 4(l)]. This latter test [along with the test of Fig. 4(i) and the fact that the result is independent of magnetic field] shows that transitions from $2^3\mathrm{P}_1(m = \pm 1)$ to $2^3\mathrm{P}_0$ (that would be possible if the microwave polarization were not perfect) do not have a significant effect on the measurement.

The measurement was performed blind (with respect to previous measurements of this interval) by adding a unknown offset (of between -4 and $+4$ kHz) to all frequencies during analysis. This fixed unknown offset was implemented more than five years ago when this work began and was revealed to the authors only after completing all of the analysis for the measurement (less than 48 hours before the submission of this work).

The weighted average of the results shown in Fig. 4(b) is $29\,616\,955\,018(15)_\mathrm{e}(6)_\mathrm{Z}(2)_\mathrm{D}$ Hz, where the uncertainties come from the extrapolations to $P = 0$ (this uncertainty is limited by statistical uncertainties), the Zeeman shift, and the Doppler shift. Adding the uncertainties in quadrature would lead to an uncertainty of 16 Hz. However, we take a more conservative tack and base our uncertainty on the proven level of consistency demonstrated for a wide range of parameters in Fig. 4, and conservatively assign a larger estimate for our one-sigma uncertainty of ± 60 Hz to our measurement. This final uncertainty is one part in 30 000 of the natural width of the $2^3\mathrm{P}$ states. For such a precise measurement, we believe that the more conservative strategy is preferred since it tries to account for the possibility of unknown systematic effects. The possible size of such unknown effects can only be limited by looking at the level of consistency as a wide range of parameters are varied. The history of large discrepancies between precision measurements (as seen, for example, in Fig. 6 [53]) justifies taking such a conservative strategy for assigning our uncertainty. Our final measurement result is

$$[E(2^3\mathrm{P}_0) - E(2^3\mathrm{P}_1)]/h = 29\,616\,955\,018(60)\ \mathrm{Hz}. \quad (2)$$

Our measured value is somewhat larger (1.6 times the estimated theoretical uncertainty) than the best theoretical prediction [48], as seen in Fig. 5. As can be seen in the figure, there are large disagreements with previous measurements. The measurement of Hu *et al.* [21] disagrees by 6.7 times their uncertainty. Our previous microwave measurement [18,23] from 22 years ago also disagrees with the

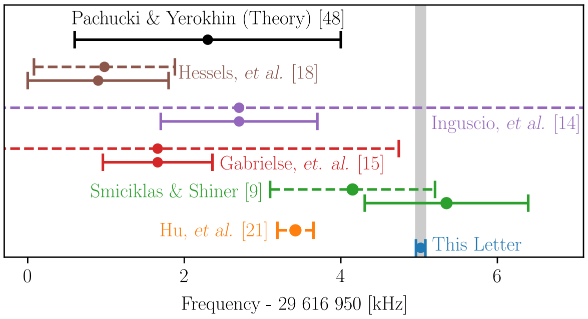

FIG. 5. A comparison of the present measurement to previous measurements [9,14,15,18,21] and to theory [48]. Corrected centers including quantum-interference effects [24,26] are also shown with dashed error bars.

present measurement (by 4.5 times the uncertainty of the previous measurement). The current work agrees with the measurement of Shiner *et al.* [9]. With the inclusion of quantum interference corrections (and the resulting expanded uncertainties) [24,26], it is also in reasonable agreement with the saturated-absorption measurement of Gabrielse *et al.* [15].

Although it is not our place to comment on measurements made by others, we will comment on the disagreement with our own previous measurement. That measurement [18] was performed without the advantages of SOF or FOSOF and therefore was limited to measuring a single Lorentzian line profile without the possibility of varying timing parameters [as was done here in Figs. 4(b)–4(d)] to search for possible systematic effects. As a result, a systematic effect (of as yet undetermined origin) must have been overlooked in that measurement. We note that if we had been as conservative then as we have chosen to be now (by expanding our 16 Hz uncertainty to 60 Hz during our blind analysis) there would have been no discrepancy between our two measurements.

Combining this measurement with our previous measurement [22] of the $J = 1$ to $J = 2$ interval leads to a determination of the $J = 0$-to-$J = 2$ interval (which is more straightforward for theory since it does not involve the 2^3P_1 state which has a singlet-state admixture):

$$[E(2^3P_0) - E(2^3P_2)]/h = 31\,908\,131\,608(65)\ \text{Hz}. \quad (3)$$

The current work is the most precise measurement to date of helium fine structure and represents a major advance in this precision. The outstanding signal-to-noise ratio has allowed for a very extensive survey of systematic effects. This work, when combined with more precise theory, could provide ppb tests of the physics and constants relevant to the interval—including a precise determination of the fine-structure constant, the most precise test of QED in a multielectron system, and tests for physics beyond the standard model. Further improvements in signal size (from a colder discharge source, a more efficient 2DMOT, higher microwave power, and more efficient laser excitation and detection) and a lower noise floor (from reduced collisional ionization due to a better vacuum) should allow for even smaller statistical uncertainties and more extensive tests for systematic effects. For our next-generation measurement, we will aim for a final uncertainty of 10 Hz or smaller, which could lead to a determination of α to 0.15 ppb.

This work is supported by NSERC, ORF, and CFI.

*hessels@yorku.ca

[1] C. Schwartz, Phys. Rev. **134**, A1181 (1964).
[2] F. M. J. Pichanick, R. D. Swift, C. E. Johnson, and V. W. Hughes, Phys. Rev. **169**, 55 (1968).
[3] A. Kponou, V. W. Hughes, C. E. Johnson, S. A. Lewis, and F. M. J. Pichanick, Phys. Rev. Lett. **26**, 1613 (1971).
[4] A. Kponou, V. W. Hughes, C. E. Johnson, S. A. Lewis, and F. M. J. Pichanick, Phys. Rev. A **24**, 264 (1981).
[5] W. Frieze, E. A. Hinds, V. W. Hughes, and F. M. J. Pichanick, Phys. Rev. A **24**, 279 (1981).
[6] D. Shiner, R. Dixson, and P. Zhao, Phys. Rev. Lett. **72**, 1802 (1994).
[7] D. L. Shiner and R. Dixson, IEEE Trans. Instrum. Meas. **44**, 518 (1995).
[8] J. Castillega, D. Livingston, A. Sanders, and D. Shiner, Phys. Rev. Lett. **84**, 4321 (2000).
[9] M. Smiciklas and D. Shiner, Phys. Rev. Lett. **105**, 123001 (2010).
[10] M. Prevedelli, P. Cancio, G. Giusfredi, F. S. Pavone, and M. Inguscio, Opt. Commun. **125**, 231 (1996).
[11] F. Minardi, G. Bianchini, P. C. Pastor, G. Giusfredi, F. S. Pavone, and M. Inguscio, Phys. Rev. Lett. **82**, 1112 (1999).
[12] P. C. Pastor, G. Giusfredi, P. De Natale, G. Hagel, C. de Mauro, and M. Inguscio, Phys. Rev. Lett. **92**, 023001 (2004).
[13] P. C. Pastor, G. Giusfredi, P. De Natale, G. Hagel, C. de Mauro, and M. Inguscio, Phys. Rev. Lett. **97**, 139903(E) (2006).
[14] G. Giusfredi, P. C. Pastor, P. De Natale, D. Mazzotti, C. d. Mauro, L. Fallani, G. Hagel, V. Krachmalnicoff, and M. Inguscio, Can. J. Phys. **83**, 301 (2005).
[15] T. Zelevinsky, D. Farkas, and G. Gabrielse, Phys. Rev. Lett. **95**, 203001 (2005).
[16] C. H. Storry and E. A. Hessels, Phys. Rev. A **58**, R8 (1998).
[17] C. H. Storry, M. C. George, and E. A. Hessels, Phys. Rev. Lett. **84**, 3274 (2000).
[18] M. C. George, L. D. Lombardi, and E. A. Hessels, Phys. Rev. Lett. **87**, 173002 (2001).
[19] J. S. Borbely, M. C. George, L. D. Lombardi, M. Weel, D. W. Fitzakerley, and E. A. Hessels, Phys. Rev. A **79**, 060503(R) (2009).
[20] G.-P. Feng, X. Zheng, Y. R. Sun, and S.-M. Hu, Phys. Rev. A **91**, 030502(R) (2015).
[21] X. Zheng, Y. R. Sun, J.-J. Chen, W. Jiang, K. Pachucki, and S.-M. Hu, Phys. Rev. Lett. **118**, 063001 (2017).
[22] K. Kato, T. D. G. Skinner, and E. A. Hessels, Phys. Rev. Lett. **121**, 143002 (2018).

[23] A. Marsman, M. Horbatsch, and E. A. Hessels, Phys. Rev. A **86**, 012510 (2012).
[24] A. Marsman, M. Horbatsch, and E. A. Hessels, Phys. Rev. A **86**, 040501(R) (2012).
[25] A. Marsman, E. A. Hessels, and M. Horbatsch, Phys. Rev. A **89**, 043403 (2014).
[26] A. Marsman, M. Horbatsch, and E. A. Hessels, Phys. Rev. A **91**, 062506 (2015).
[27] A. Marsman, M. Horbatsch, and E. A. Hessels, J. Phys. Chem. Ref. Data **44**, 031207 (2015).
[28] B. Schiff, C. L. Pekeris, and H. Lifson, Phys. Rev. **137**, A1672 (1965).
[29] K. Y. Kim, Phys. Rev. **140**, A1498 (1965).
[30] L. Hambro, Phys. Rev. A **5**, 2027 (1972).
[31] L. Hambro, Phys. Rev. A **6**, 865 (1972).
[32] L. Hambro, Phys. Rev. A **7**, 479 (1973).
[33] M. Douglas and N. M. Kroll, Ann. Phys. (N.Y.) **82**, 89 (1974).
[34] J. Daley, M. Douglas, L. Hambro, and N. M. Kroll, Phys. Rev. Lett. **29**, 12 (1972).
[35] M. L. Lewis and P. H. Serafino, Phys. Rev. A **18**, 867 (1978).
[36] Z.-C. Yan and G. W. F. Drake, Phys. Rev. Lett. **74**, 4791 (1995).
[37] T. Zhang, Phys. Rev. A **54**, 1252 (1996).
[38] T. Zhang, Phys. Rev. A **53**, 3896 (1996).
[39] T. Zhang, Z.-C. Yan, and G. W. F. Drake, Phys. Rev. Lett. **77**, 1715 (1996).
[40] G. W. F. Drake, Can. J. Phys. **80**, 1195 (2002).
[41] K. Pachucki and J. Sapirstein, J. Phys. B **33**, 5297 (2000).
[42] K. Pachucki and J. Sapirstein, J. Phys. B **36**, 803 (2003).
[43] J. Sapirstein, J. Phys. B **43**, 074015 (2010).
[44] K. Pachucki, J. Phys. B **32**, 137 (1999).
[45] K. Pachucki, Phys. Rev. Lett. **97**, 013002 (2006).
[46] K. Pachucki and V. A. Yerokhin, Phys. Rev. A **79**, 062516 (2009).
[47] K. Pachucki and V. A. Yerokhin, Phys. Rev. A **80**, 019902(R) (2009).
[48] K. Pachucki and V. A. Yerokhin, Phys. Rev. Lett. **104**, 070403 (2010).
[49] K. Pachucki and V. A. Yerokhin, Can. J. Phys. **89**, 95 (2011).
[50] K. Pachucki and V. A. Yerokhin, J. Phys. Conf. Ser. **264**, 012007 (2012).
[51] Z. Pei-Pei, Z. Zhen-Xiang, Y. Zong-Chao, and S. Ting-Yun, Chin. Phys. B **24**, 033101 (2015).
[52] J. Lifsitz, *A Measurement of the Triplet-2P Fine Structure of Helium-4* (University of Michigan Thesis, Ann Arbor, 1965).
[53] See Supplemental Material at http://link.aps.org/supplemental/10.1103/PhysRevLett.132.163001 for figures that set the context for this measurement.
[54] K. Pachucki, V. Patkóš, and V. A. Yerokhin, Phys. Rev. A **95**, 062510 (2017).
[55] F. Ficek, D. F. Jackson, M. G. Kozlov, N. Leefer, S. Pustelny, and D. Budker, Phys. Rev. A **95**, 032505 (2017).
[56] X. Fan, T. G. Myers, B. A. D. Sukra, and G. Gabrielse, Phys. Rev. Lett. **130**, 071801 (2023).
[57] T. Aoyama, M. Hayakawa, T. Kinoshita, and M. Nio, Phys. Rev. Lett. **109**, 111807 (2012).
[58] S. Laporta, Phys. Lett. B **772**, 232 (2017).
[59] T. Aoyama, T. Kinoshita, and M. Nio, Phys. Rev. D **97**, 036001 (2018).
[60] S. Volkov, Phys. Rev. D **100**, 096004 (2019).
[61] R. H. Parker, C. Yu, W. Zhong, B. Estey, and H. Müller, Science **360**, 191 (2018).
[62] R. Bouchendira, P. Cladé, S. Guellati-Khélifa, F. Nez, and F. Biraben, Phys. Rev. Lett. **106**, 080801 (2011).
[63] G. Gabrielse, S. F. Hoogerheide, J. Dorr, and E. Novitski, in *Fundamental Physics in Particle Traps* (Springer, New York, 2014), pp. 1–40.
[64] Y. Kahn, G. Krnjaic, S. Mishra-Sharma, and T. M. P. Tait, J. High Energy Phys. 05 (2017) 002.
[65] C. Bœhm and J. Silk, Phys. Lett. B **661**, 287 (2008).
[66] A. C. Vutha and E. A. Hessels, Phys. Rev. A **92**, 052504 (2015).
[67] N. F. Ramsey, Phys. Rev. **76**, 996 (1949).
[68] Z.-C. Yan and G. W. F. Drake, Phys. Rev. A **50**, R1980 (1994).
[69] S. A. Lewis, F. M. J. Pichanick, and V. W. Hughes, Phys. Rev. A **2**, 86 (1970).